Catalysis Science & Technology

Accepted Manuscript

ROYAL SOCIETY OF CHEMISTRY

www.rsc.org/catalysis

Table of Content:

Highly Selective and Efficient Acetalization of Aldehydes and Ketones Catalyzed by Heterogeneous Catalyst of $H_4[SiW_{12}O_{40}]/SiO_2$

Shen Zhao, Yueqing Jia and Yu-Fei Song*

State Key Laboratory of Chemical Resource Engineering, Beijing University of Chemical Technology, Beijing 100029, P. R. China.

It has been demonstrated that $H_4[SiW_{12}O_{40}]$ (H-SiW_{12}) is able to catalyze the acetalization of aldehydes and ketones with ethylene glycol and 1,3-propanediol efficiently. Nevertheless, the possible leaching and the recycling of H-SiW_{12} restrict its further application. The immobilization of $H_4[SiW_{12}O_{40}]$ onto SiO_2 leads to the heterogeneous catalyst of $H_4[SiW_{12}O_{40}]/SiO_2$ (H-SiW_{12}/SiO_2), which can catalyze acetalization of aldehydes and ketones with ethylene glycol and 1,3-propanediol selectively and efficiently without drying agents. The acetalization process can proceed smoothly at relative low temperature under solvent-free conditions. Moreover, $H_4[SiW_{12}O_{40}]/SiO_2$ can be recycled at least ten times without obvious decrease of catalytic activity. The TONs of H-SiW_{12}/SiO_2-catalyzed acetalization of cyclohexanone with ethylene glycol, and benzaldehyde with 1,3-propanediol are the highest one reported so far.

Keywords: polyoxometalates, acetalization, Brónsted acid, immobilization

Catalysis Science & Technology RSCPublishing

ARTICLE

Acetalization of Aldehydes and Ketones over $H_4[SiW_{12}O_{40}]$ and $H_4[SiW_{12}O_{40}]/SiO_2$

Cite this: DOI: 10.1039/x0xx00000x

Shen Zhao,† Yueqing Jia,† Yu-Fei Song*

Received
Accepted

DOI: 10.1039/x0xx00000x

www.rsc.org/

The $H_4[SiW_{12}O_{40}]$ (H-SiW_{12}) is demonstrated to be able to catalyze the acetalization of aldehydes and ketones with ethylene glycol and 1,3-propanediol efficiently. Nevertheless, the possible leaching and the recycling of H-SiW_{12} are two major disadvantages that large restrict its further application in industry. Moreover, $H_4[SiW_{12}O_{40}]$ tends to deactivate strong proton sites due to the small surface area of 10 $m^2 \cdot g^{-1}$. Due to the interactions with surface silanol groups, the proton sites of polyoxometalates (POMs) on SiO_2 are less susceptible to deactivate. As such, immobilization of $H_4[SiW_{12}O_{40}]$ onto SiO_2 leads to the heterogeneous catalyst of $H_4[SiW_{12}O_{40}]/SiO_2$ (H-SiW_{12}/SiO_2), which can catalyze acetalization of aldehydes and ketones with ethylene glycol and 1,3-propanediol selectively and efficiently without drying agents. The acetalization process can proceed smoothly at relative low temperature under solvent-free conditions. The catalyst of $H_4[SiW_{12}O_{40}]/SiO_2$ can be recycled at least ten times without obvious decrease of catalytic activity. As far as we know, the TONs of H-SiW_{12}/SiO_2-catalyzed acetalization of cyclohexanone with ethylene glycol, and benzaldehyde with 1,3-propanediol are the highest one reported so far.

1. Introduction

Acetalization of aldehydes and ketones with alcohols or diols is a widely used approach in pharmaceutical industries such as drug design and carbohydrate chemistry *etc*,[1-3] the currently used catalysts for acetalization of aldehydes and ketones include HCl, *tri*-fluoroacetic acid (TFA) and *p*-toluenesulfonic acid (*p*-TSA)[4], solid acids,[5,6] functionalized silica,[7-9] acidic polymers,[10,11] Lewis acids,[12] metal catalysts,[13-16] organocatalysts,[17] and kaolintic clay[18]. However, the reported catalytic systems show the following disadvantages and potential technological and environmental problems, which, in the long run, cannot meet the green and sustainable requirement because that (1) the used inorganic acids such as H_2SO_4, HCl, *p*-toluenesulfonate *etc* are corrosive; (2) the excess of amount of drying agents such as silical gel, montmorillonite and molecular sieve *etc* are needed; and (3) the selectivity is usually poor. As such, it is significant to develop reusable, environmental-benign, selective and efficient green catalysts without drying agents.

Polyoxometalates (POMs) are a large family of anionic metal-oxides of V, Mo, W and Nb *etc.* POMs have demonstrated to be attractive acid catalysts[21-26] for hydration,[27,28] esterification,[29,30] acetoxylation,[31,32] isomerization,[33,34] saccharification[35,36] and cycloaddition[37] *etc*, due to the stronger acidity, Keggin POMs generally exhibit much higher catalytic activities compared to conventional catalysts, such as mineral acids, ion-exchange resins, mixed oxides, zeolites, *etc*. Unlike the network structure of zeolites and metal oxides, POMs possess the discrete ionic structures, which endow POMs extremely high proton mobility and a “pseudo-liquid phase”. On top of that, POMs are thermally and oxidatively stable compared with commonly used organic ligands.[21-26] As such, POMs are superior candidates as acid catalysts for acetalization.

In this paper, the Keggin cluster of $H_4[SiW_{12}O_{40}]$ (H-SiW_{12}) has been developed to catalyze acetalization of aldehydes and ketones under solvent-free conditions. Selective and efficient acetalization of aldehydes and ketones can be achieved by H-SiW_{12} without drying agents under mild conditions. Furthermore, the immobilization of H-SiW_{12} onto SiO_2 results in the formation of the heterogeneous catalyst of H-SiW_{12}/SiO_2,[38] which have shown selective and efficient acetalization of aldehydes and ketones. In addition, H-SiW_{12}/SiO_2 is truly heterogeneous and can be recycled at least ten times without obvious decrease of catalytic activity, and the recycled catalyst of H-SiW_{12}/SiO_2 remains its structure and composition.

2. Experimental Section

2.1. Chemicals

Cyclohexanone (99%), 2-adamantanone (98%), hexanal (99%), heptanal (99%), octanal (98%), nonanal (99%), decanal (96%), cyclohexanecarboxaldehyde (98%), benzaldehyde (98%), 2-methylbenzaldehyde (98%), 3-methylbenzaldehyde (97%), 4-methylbenzaldehyde (98%), 2-methoxybenzaldehyde (98%), 3-methoxybenzaldehyde (98%), 4-methoxybenzaldehyde (98%), 2-chlorobenzaldehyde (97%), 3-chlorobenzaldehyde (97%), 4-chlorobenzaldehyde (98%), 2-bromobenzaldehyde (98%), 3-bromobenzaldehyde (97%), 4-bromobenzaldehyde (99%), 2-nitrobenzaldehyde (98%), 3-nitrobenzaldehyde (99%), 4-nitrobenzaldehyde (99%), ethylene glycol (99%), 1,3-propanediol (99%), and all solvents were purchased from Alfa Aesar. Analytical silicotungstic acid ($H_4SiW_{12}O_{40}$) was obtained from Energy Chemical in Shanghai. Silica gel (SiO_2, pore size: 6 nm, particle size: 40-63 μm) was purchased from Sigma Aldrich. All the chemicals and solvents were used without further purification.

2.2. Measurements

Powder X-ray diffraction (XRD) patterns were recorded on a Rigaku XRD-6000 diffractometer under the following conditions: 40 kV, 30 mA, Cu Kα radiation (λ = 0.154 nm). Fourier transform infrared (FT-IR) spectra were recorded on a Bruker Vector 22 infrared spectrometer using KBr pellet method. Inductively coupled plasma-atomic emission spectroscopy (ICP-AES) analysis was performed using a Shimadzu ICPS-7500 spectrometer. BET measurements were performed at 77 K on a Quantachrome Autosorb-1C analyzer. The samples were degassed at 110 °C for 6 hours before the measurements. Solid state NMR measurements were carried out on a Bruker Avance 300 M solid-state spectrometer equipped with a commercial 7 mm MAS NMR probe. X-ray photoelectron spectroscopy (XPS) measurements were performed with mono-chromatized Al Kα exciting X-radiation (PHI Quantera SXM). Temperature-programmed desorption of ammonia (NH_3-TPD) was performed using Auto Chem. II 2920 equipment. The corresponding acetals and ketals were analyzed by Agilent 7820A gas chromatography (GC) system using a 30 m 5% phenylmethyl silicone capillary column with an ID of 0.32 mm and 0.25 μm coating (HP-5). Yields were determined by GC analysis using reference standards. Assignments of the corresponding acetals and ketals were analyzed by ^{1}H-NMR spectra recorded on a Bruker 400 MHz NMR spectrometer.

2.3. Synthesis of H-SiW$_{12}$/SiO$_2$

$H_4SiW_{12}O_{40}$ (1 g) was dissolved in 50 ml H_2O, which was added to SiO_2 (10g) suspended in 50 ml H_2O. The resulting mixture was stirred at 25 °C overnight and H_2O was evaporated under vacuum. The obtained H-SiW$_{12}$/SiO$_2$ was dried under reduced pressure overnight. ICP analysis showed that the 9.0 wt.% $H_4SiW_{12}O_{40}$ on the SiO_2 support. The specific surface area determined by BET method is 324 $m^2 g^{-1}$. The average pore diameter and the single-point total pore volume are 6.6 nm and 0.67 $cm^3 g^{-1}$, respectively.

2.4. Procedure for the acetalization of aldehydes and ketones

In a typical experiment, 1 mmol aldehyde or ketone, 1.5 mmol ethylene glycol or 1,3-propanediol and H-SiW$_{12}$/SiO$_2$ (0.225 μmol H-SiW$_{12}$) as catalyst were placed in a 20 ml glass bottle at 60 °C and the reaction mixture was kept stirring vigorously. The reaction was effectively quenched after 6 hours. The resulting oily products were extracted by diethyl ether, analyzed by GC, and identified by ^{1}H-NMR. The yields were determined by reference standards. After completion of the reaction, H-SiW$_{12}$/SiO$_2$ were recovered by centrifugation, washed with acetone, and dried in air.

3. Results and Discussion

3.1. Catalysis of H-SiW$_{12}$

Table 1. The effect of different catalysts on acetalization of cyclohexanone with ethylene glycol at 25 °C under solvent-free condition.[a]

Entry	Catalyst	Yield(%)
1	H-SiW$_{12}$	92
2	K-PW$_{11}$	<0.1
3	K-SiW$_{11}$	<0.1
4	Na-A-PW$_9$	<0.1
5	Na-B-PW$_9$	<0.1
6	Na-SiW$_9$	<0.1
7	K-W$_2$	<0.1
8	K-La(PW$_{11}$)$_2$	<0.1
9	K-Ce(PW$_{11}$)$_2$	<0.1
10	Na_2WO_4	<0.1
11	Na_2SiO_3	<0.1
12	Na_2HPO_4	<0.1
13	NaH_2PO_4	<0.1
14	WO_3	<0.1
15	None	<0.1

[a] Reaction conditions: cyclohexanone (1 mmol), catalyst (5.5 mol% based on W to cyclohexanone), ethylene glycol (1.5 mmol), 25 °C, 6 hours. Yields were determined by GC analysis using reference standard. Assignments of corresponding products were analyzed by ^{1}H-NMR.

As the first trial, the acetalization of cyclohexanone with ethylene glycol catalyzed by H-SiW$_{12}$ has been carried out under solvent-free conditions. It is found that good yield of 92% with excellent selectivity of above 99.9% can be obtained in 6 hours at 25 °C (Table 1, Entry 1). Contrast experiments under the same conditions suggest that the lacunary Keggin clusters of $K_7[PW_{11}O_{39}]$ (K-PW$_{11}$), $K_8[SiW_{11}O_{39}]$ (K-SiW$_{11}$), $Na_8H[A\text{-}PW_9O_{34}]$ (Na-A-PW$_9$), $Na_8H[B\text{-}PW_9O_{34}]$ (Na-B-PW$_9$) and $Na_{10}[SiW_9O_{34}]$ (Na-SiW$_9$) are not effective (Entries 2-6) for such acetalization. Furthermore, the $K_2[\{WO(O_2)_2(H_2O)\}_2(\mu\text{-}O)]\cdot 2H_2O$ (K-W$_2$) is not effective too (Entry 7). The lanthanide-containing POMs of $K_{11}[La(PW_{11}O_{39})_2]$ (K-La(PW$_{11}$)$_2$) and $K_{11}[Ce(PW_{11}O_{39})_2]$ (K-Ce(PW$_{11}$)$_2$), involving Lewis-acid center of La^{3+} and Ce^{3+}, have not shown any catalytic activities (Entries 8-9). In addition, Na_2WO_4, Na_2SiO_3, Na_2HPO_4, NaH_2PO_4 and WO_3 are not effective either (Entries 10-14). The reaction hardly proceeds in the absence of the catalyst (Entry 15). The above experimental results clearly indicate that the Brónsted-acid catalyst of H-SiW$_{12}$ is selective and effective for acetalization of cyclohexanone. On the basis of the first trial, it is reasonable to extend the substrates towards a wide range of aldehydes and ketones.

The acetalization of 2-methylbenzaldehyde with ethylene glycol using H-SiW$_{12}$ as catalyst has been performed, and it is noted that the yield is quite low at 25 °C under solvent-free conditions. As such, the effect of temperature (denoted as T) on acetalization is explored. As shown in Figure 1A, for 2-methylbenzaldehyde, the yield increases from 49% to 81% upon increasing T from 25 to 60 °C, and the yield remains unchanged by further increase T from 60 to 70 °C. For cyclohexanone, the yield remains almost the same upon increasing T from 25 to 70 °C. In order to explain the catalytic results in detail, the kinetic parameters for acetalization of cyclohexanone and 2-methylbenzaldehyde with ethylene glycol catalyzed by H-SiW$_{12}$ have been calculated. In addition, the yield and ln(C_t/C_0) are plotted against reaction time at 25 °C, 40 °C, 50 °C, 60 °C and 70 °C (Fig S1 and S2), in which C_0 and C_t are concentrations of cyclohexanone ketal or 2-methylbenzaldehyde acetal at initial time (t =0) and time t, respectively. The linear fit of data reveals the pseudo-first-order kinetics for acetalization of cyclohexanone and 2-methylbenzaldehyde with ethylene glycol at different temperatures. Figure 1B shows the plot of lnk(T) *vs* (-1/T). The calculated activation energy (E_a) by Arrhenius equation for acetalization of cyclohexanone and 2-methylbenzaldehyde with ethylene glycol are 3.3 and 15.9 kJ·mol^{-1}, respectively. The E_a for acetalization of cyclohexanone with ethylene glycol is much lower than that for that of 2-methylbenzaldehyde with ethylene glycol. The above result can explain the differences between acetalization of cyclohexanone and 2-methylbenzaldehyde with ethylene glycol at different temperatures. Furthermore, the yields and E_a for acetalization of various substrates with ethylene glycol catalyzed by H-SiW$_{12}$ have been summarized in Table S4. The yields at 60 °C are much higher than that at 25 °C in most cases. Therefore, the acetalization of various aldehydes and ketones with ethylene glycol and 1,3-propanediol has been performed at 60 °C in order to achieve good yields using H-SiW$_{12}$ as catalyst.

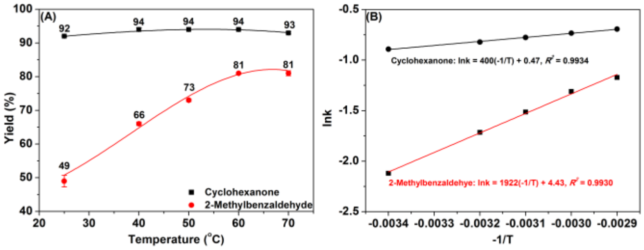

Figure 1. Effect of temperature on acetalization of cyclohexanone and 2-methylbenzaldehyde with ethylene glycol (A) and the plot lnk(T) vs (-1/T). Reaction conditions: cyclohexanone or 2-methylbenzaldehyde (1 mmol), H-SiW$_{12}$ (0.25 mol% to cyclohexanone or 2-methylbenzaldehyde), ethylene glycol (1.5 mmol), 6 hours.

$$-dC_t / dt = kC_t \qquad (1)$$

$$\ln(C_t / C_o) = -kt \qquad (2)$$

$$\ln k = (\ln A - E_a) / RT \qquad (3)$$

As shown in Table 2 and Table S5, H-SiW$_{12}$ can realize selective and efficient acetalization of various aldehydes and ketones with ethylene glycol or 1,3-propanediol, and all the corresponding acetals and ketals can be afforded in good yields with excellent selectivity of all above 99.9%.

The above results reveal that H-SiW$_{12}$ can catalyze the acetalization of various aldehydes and ketones with ethylene glycol and 1,3-propanediol selectively and efficiently. However, the ICP analysis of reaction filtrate after acetalization of benzaldehyde with 1,3-propanediol catalyzed by H-SiW$_{12}$ reveal the contents of Si and W are 0.04 and 0.49 ppm, respectively (Table S7). The ICP results clearly show that H-SiW$_{12}$ is partly dissolved in reaction mixture during the catalytic reaction, which means the H-SiW$_{12}$ is leaching during the reaction. Therefore, the leaching of H-SiW$_{12}$ and the recycling of H-SiW$_{12}$ are potential problems for its further application.[27] Moreover, H-SiW$_{12}$ tends to deactivate strong proton sites due to the small surface area of 10 m^2 g^{-1}. In this regard, SiO$_2$ is the ideal support for H-SiW$_{12}$ for its large surface area and inertness towards Keggin POMs. Due to the interaction with surface silanol groups, the proton sites of POMs/SiO$_2$ are less susceptible to deactivate.[26] As such, immobilization of H-SiW$_{12}$ onto SiO$_2$ leads to the formation of heterogeneous catalyst of H-SiW$_{12}$/SiO$_2$.[38]

Table 2. Acetalization of various aldehydes and ketones with ethylene glycol catalyzed by H-SiW$_{12}$ at 60 °C under solvent-free conditions.[a]

Entry	Donor	Acceptor	Product	Yield(%)
		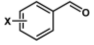	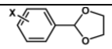	
1		X = H	X = H	73
2		X = 2-Me	X = 2-Me	81
3		X = 3-Me	X = 3-Me	73
4		X = 2-Cl	X = 2-Cl	95
5		X = 3-Cl	X = 3-Cl	90
6		X = 4-Cl	X = 4-Cl	80
7		X = 2-Br	X = 2-Br	93
8		X = 3-Br	X = 3-Br	85
9		X = 4-Br	X = 4-Br	89
10		X = 2-NO$_2$	X = 2-NO$_2$	93
11		X = 3-NO$_2$	X = 3-NO$_2$	94
12	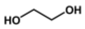	X = 4-NO$_2$	X = 4-NO$_2$	>99.9
		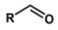	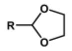	
13		R = n-C$_5$H$_{11}$	R = n-C$_5$H$_{11}$	>99.9
14		R = n-C$_6$H$_{13}$	R = n-C$_6$H$_{13}$	98
15		R = n-C$_7$H$_{15}$	R = n-C$_7$H$_{15}$	99
16		R = n-C$_8$H$_{17}$	R = n-C$_8$H$_{17}$	99
17		R = n-C$_9$H$_{19}$	R = n-C$_9$H$_{19}$	98
18		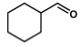	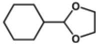	97
19		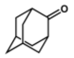	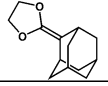	99

[a] Reaction conditions: substrate (1 mmol), H-SiW$_{12}$ (0.25 mol% to substrate), ethylene glycol (1.5 mmol), 60 °C, 6 hours. Yields were determined by GC analysis using reference standards. Assignments of corresponding products were analyzed by ^{1}H-NMR.

3.2. Characterization of H-SiW$_{12}$/SiO$_2$

Table 3. BET and NH_3-TPD results of H-SiW_{12}/SiO_2, SiO_2 and H-SiW_{12}.

Entry	Catalyst	Surface Area ($m^2 \cdot g^{-1}$)	Pore Volume ($cm^3\ g^{-1}$)	Pore Size (nm)	Total Acidity (mmol NH_3 $gcat^{-1}$)[a]
1	SiO_2	490	0.82	6.6	-
2	fresh H-SiW_{12}/SiO_2	324	0.67	6.6	0.42
3	reused H-SiW_{12}/SiO_2	322	0.66	6.5	0.41
4	H-SiW_{12}	9	0.026	0.4	0.44

[a] The amount of acid sites were calculated by quantifying the desorbed NH_3 from NH_3-TPD.

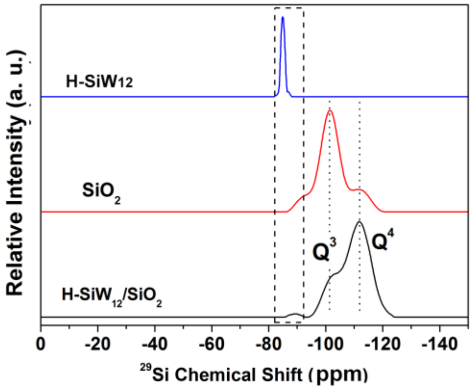

Figure 2. ^{29}Si CP/MAS NMR spectra of H-SiW_{12}/SiO_2, SiO_2 and H-SiW_{12}.

ICP analysis of H-SiW_{12}/SiO_2 shows 9.0 wt.% $H_4SiW_{12}O_{40}$ on the SiO_2 support (Table S1). Powder XRD pattern of H-SiW_{12}/SiO_2 reveals the characteristic peak of H-SiW_{12} at 2θ = 8.46°, which reveals that the structure of H-SiW_{12} remains unchanged after being immobilized onto the SiO_2 support (Fig S3A). The weak resonance compared with that of the H-SiW_{12} is due to the fact that only 9.0 wt. % H-SiW_{12} has been immobilized onto SiO_2. FT-IR spectrum of H-SiW_{12} shows four characteristic peaks of W-O stretching bands at 934, 891, 790, and 715 cm^{-1}, which have shifted to 935, 893, 792, and 716 cm^{-1} in the corresponding FT-IR spectrum of H-SiW_{12}/SiO_2, respectively (Fig S3B). These shifts reveal the presence of the hydrogen bonding interactions between the hydroxyl groups on the surface of SiO_2 support and the oxygen atoms of the H-SiW_{12}.

As shown in Fig 3, the ^{29}Si CP/MAS NMR spectrum of H-SiW_{12}/SiO_2 exhibits two resonances at -102.8 and -111.9 ppm, which correspond to $(SiO)_3SiOH$ (Q^3) and $Si(OSi)_4$ (Q^4). At the same time, SiO_2 also exhibits Q^3 and Q^4 peaks at -101.5 and 110.8 ppm. It should be noted that the Q^4 peak is the main peak in the ^{29}Si CP/MAS NMR spectrum of H-SiW_{12}/SiO_2, whereas the Q^3 peak is the main peak in the ^{29}Si CP/MAS NMR spectrum of SiO_2. Such differences can be explained by the fact that H-SiW_{12} is bound to SiO_2 through the hydrogen bonding interactions.[39] The ^{29}Si CP/MAS NMR spectrum of H-SiW_{12} shows one peak at -84.9 ppm, while that of H-SiW_{12}/SiO_2 at -86.0 ppm. The weak resonance compared with that of the H-SiW_{12} is due to the fact that only 9.0 wt. % H-SiW_{12} has been immobilized onto SiO_2. The peak shift is due to the hydrogen bonding interactions between the hydroxyl groups on SiO_2 support and the oxygen atoms of the H-SiW_{12}.

XPS spectra corresponding to W core levels of the H-SiW_{12}/SiO_2 and H-SiW_{12} are shown in Fig 3A. The binding energy of $W4f_{7/2}$ and $W4f_{5/2}$ are 36.4 and 38.1 eV for H-SiW_{12}/SiO_2, and 36.2 and 37.8 eV for H-SiW_{12}. XPS spectra corresponding to Si core levels of the H-SiW_{12}/SiO_2 and SiO_2 are shown in Fig 3B. The Si2p peak at 101.2 eV in the H-SiW_{12} is so weak that the Si2p peak of H-SiW_{12} will be overlapped by the Si2p peak of SiO_2 in the H-SiW_{12}/SiO_2 as only 9.0 wt. % H-SiW_{12} has been immobilized onto SiO_2. Therefore, the Si2p peak in the H-SiW_{12}/SiO_2 comes from SiO_2 not from H-SiW_{12}. The binding energy of Si2p is 103.1 eV in H-SiW_{12}/SiO_2, and 102.8 eV in SiO_2. The above results reveal that the binding energy of $W4f_{7/2}$ and $W4f_{5/2}$ in the H-SiW_{12}/SiO_2 are higher than those of the H-SiW_{12}, and the binding energy of Si2p in the H-SiW_{12}/SiO_2 is higher than those of the SiO_2. These results confirm the presence of the hydrogen bonding interactions between the hydroxyl groups on SiO_2 support and the oxygen atoms of the H-SiW_{12} in the H-SiW_{12}/SiO_2.

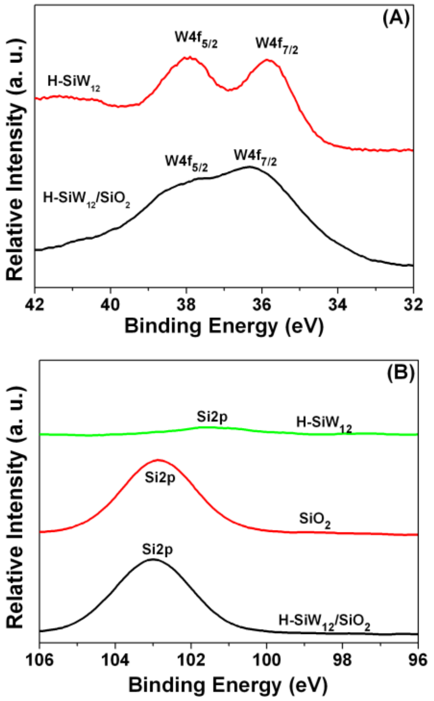

Figure 3. XPS spectra of H-SiW_{12}/SiO_2, SiO_2 and H-SiW_{12}.

BET measurements have been performed on H-SiW_{12}/SiO_2, SiO_2 and H-SiW_{12}, and the specific surface area, pore volume, and pore diameters are presented in Table 3. The samples of H-

SiW_{12}/SiO_2 and SiO_2 display a type IV isotherm with H_1 hysteresis (Fig S4A).[40] The SiO_2 exhibits a maximum pore diameter of 6.6 nm and surface area of 490 $m^2 \cdot g^{-1}$. The H-SiW_{12}/SiO_2 remains the pore diameter of 6.6 nm and a decrease in surface area of 324 $m^2 \cdot g^{-1}$. The above results reveal that the immobilization of H-SiW_{12} onto SiO_2 affects the surface area and pore distribution of SiO_2. However, the surface area of H-SiW_{12}/SiO_2 (324 $m^2 \cdot g^{-1}$) is much larger than that of H-SiW_{12} (10 $m^2 \cdot g^{-1}$), which can reduce the deactivation of strong proton sites.

The above catalytic results reveal that the strong acidity of H-SiW_{12} plays a significant role in acetalization of aldehydes and ketones with ethylene glycol and 1,3-propanediol. Therefore, the acidity of the H-SiW_{12}/SiO_2 is expected to play a key role in determining the catalytic performance in acetalization of aldehydes and ketones with diols. As such, temperature-programmed desorption of ammonia (NH_3-TPD) demonstrate that the H-SiW_{12}/SiO_2 and H-SiW_{12} exhibit a main NH_3 desorption peak at 454.2 °C in Fig S5, which corresponds to the NH_3 molecules adsorbed on strong acid sites of Keggin.[41] The total acidity of the H-SiW_{12}/SiO_2 and H-SiW_{12} determined by NH_3-TPD are summarized in Table 3. The results reveal that not only H-SiW_{12} but also H-SiW_{12}/SiO_2 can provide strong acidity to promote acetalization of aldehydes and ketones with diols.

Table 4. Acetalization of various aldehydes and ketones with ethylene glycol catalyzed by heterogeneous catalyst of H-SiW_{12}/SiO_2 at 60 °C under solvent-free conditions.[a]

Entry	Donor	Acceptor	Product	Yield(%)[b]
		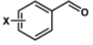	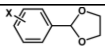	
1		X = H	X = H	73(70)
2		X = 2-Me	X = 2-Me	81(76)
3		X = 3-Me	X = 3-Me	73(69)
4		X = 2-Cl	X = 2-Cl	95(91)
5		X = 3-Cl	X = 3-Cl	90(85)
6		X = 4-Cl	X = 4-Cl	80(74)
7		X = 2-Br	X = 2-Br	93(90)
8		X = 3-Br	X = 3-Br	85(81)
9		X = 4-Br	X = 4-Br	89(86)
10		X = 2-NO_2	X = 2-NO_2	93(91)
11		X = 3-NO_2	X = 3-NO_2	94(89)
12	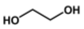	X = 4-NO_2	X = 4-NO_2	>99.9(98)
		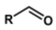	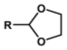	
13		R = n-C_5H_{11}	R = n-C_5H_{11}	>99.9(99)
14		R = n-C_6H_{13}	R = n-C_6H_{13}	98(96)
15		R = n-C_7H_{15}	R = n-C_7H_{15}	99(97)
16		R = n-C_8H_{17}	R = n-C_8H_{17}	99(95)
17		R = n-C_9H_{19}	R = n-C_9H_{19}	98(94)
18		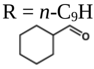	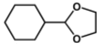	97(92)
19		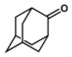	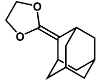	99(94)

[a] Reaction conditions: substrate (1 mmol), H-SiW_{12}/SiO_2 (0.0225 mol% to substrate), ethylene glycol (1.5 mmol), 60 °C, 6 hours. Yields were determined by GC analysis using reference standards. Assignments of corresponding products were analyzed by ^{1}H-NMR. [b] The values in parentheses are the isolated yields.

3.3. Catalysis of H-SiW_{12}/SiO_2

Acetalization of various aldehydes and ketones with ethylene glycol by H-SiW_{12}/SiO_2 at 60 °C has been investigated under solvent-free conditions. All the corresponding acetals and ketals can be afforded in good yields with excellent selectivity of above 99%. For example, benzaldehyde can be converted to the corresponding acetal in the yield of 73% (Table 4, Entry 1). Methyl-substituted aromatic aldehydes including 2-methylbenzaldehyde and 3-methylbenzaldehyde can be converted to the corresponding acetals in the yields of 81% and 73%, respectively (Entries 2-3). For cholor-, bromo- or nitro-substituted aldehydes, good yields in the range of 80~99.9% can be achieved (Entries 4-12). The above results reveal that acetalization of aromatic aldehydes with electron-drawing groups (cholor-, bromo- or nitro- substituted aldehydes) gives higher yields than those of aromatic aldehydes with electron-drawing groups (2-methylbenzaldehyde and 3-methylbenzaldehyde). The reason is that the protonation of carbonyl groups in electron-drawing substituted aromatic aldehydes is easier and more completely than that in electron-donating one. The above results confirm that the protonation of carbonyl group is essential for acetalization.

For aliphatic aldehydes, acetalization of alkyl aldehydes leads to excellent yields of >98% (Entries 13-17). Acetalization of cyclohexanecarboxaldehyde proceeds efficiently with yield of 97% (Entry 18). In terms of 2-admantanone, excellent yield of 99% can be obtained (Entry 19).

As shown in Table S6, H-SiW_{12}/SiO_2 can realize selective and efficient acetalization of various aldehydes and ketones with 1,3-propanediol, and all the corresponding acetals and ketals can be afforded in good yields with excellent selectivity of all above 99.9%.

Though acetalization of benzaldehyde with ethylene glycol over heterogeneous catalyst of $[Hmim]_3PW_{12}O_{40}$ has been reported with the high yield of 97%, the turnover number (TON) is only 111 (Table 5, Entry 4)[6], which is much lower than that of H-SiW_{12}/SiO_2 (TON = 3243, benzaldehyde: ethylene glycol: H-SiW_{12} = 4443: 6664: 1). Furthermore, the reaction condition of $[Hmim]_3PW_{12}O_{40}$ is environmental-unfriendly using toluene as solvent at 110 °C. In contrast, when H-SiW_{12}/SiO_2 is applied as catalyst, although acetalization of cyclohexanone with ethylene glycol (cyclohexanone: ethylene glycol: H-SiW_{12} = 36000: 54000: 1) proceeds in 83% yield, it is worth noting that the reaction is carried out under solvent-free conditions at 60 °C and the TON can reach as high as 29880 (Table 5, Entry 1). The TON for H-SiW_{12}/SiO_2-catalyzed acetalization of cyclohexanone with ethylene glycol is the highest one reported so far, when compared with those of SO_3H-FSM[7], SC-34-SO_3H[14], M-ZrPO[9], $Bi(OTf)_3 \cdot 4H_2O$[15], tin(IV) phosphate[16] and m-SZ[20] (Table 5, Entries 5-10).

It is worth noting that the acetalization of benzaldehyde with 1,3-propanediol proceeds efficiently in 85% yield with H-SiW_{12}/SiO_2 (benzaldehyde: H-SiW_{12} = 36000: 54000: 1) under solvent-free conditions (Table 5, Entry 2). The turnover number (TON) can reach as high as 30600. As far as we know, the

Table 5. Comparison of yields and TONs for the acetalization catalyzed by different catalysts.

Entry	Catalyst	Substrate	Alcohol	Solvent	Temp.(°C)	Time(h)	Yield(%)	TON[a]	Ref.
1	H-SiW_{12}/SiO_2	cyclohexanone	ethylene glycol	none	60	6	83	29800	this work
2	H-SiW_{12}/SiO_2	benzaldehyde	1,3-propanediol	none	60	6	85	30600	this work
3	*m*PMF[b]	benzaldehyde	1,3-propanediol	none	25	24	94	-	11
4	$[Hmim]_3PW_{12}O_{40}$	benzaldehyde	ethylene glycol	toluene	reflux	2	97	111	6
5	SO_3H-FSM[c]	cyclohexanone	ethylene glycol	toluene	reflux	10	93	930	7
6	M-ZrPO[d]	cyclohexanone	ethylene glycol	none	120	2	98	666	14
7	SC-34-SO_3H[e]	cyclohexanone	ethylene glycol	cyclohexane	90	5	98	-	9
8	$Bi(OTf)_3{\cdot}4H_2O$	cyclohexaone	ethylene glycol	toluene	110	4	82	82	15
9	tin(IV) phosphate	cyclohexanone	ethylene glycol	toluene	110	3	68	59	16
10	$Al(OTf)_3$	4-methoxybenzaldehyde	methanol	none	25	1	98	98	13
11	IL[f]	2-chlorobenzaldehyde	methanol	none	25	24	96	19	10
12	fluorous hydrazine-1,2-bis(carbothioate)	3-phenylpropionaldehyde	methanol	none	25	1	88	18	17
13	IL-silica-polymer[g]	benzaldehyde	methanol	none	30	0.6	97	388	8
14	m-SZ[h]	cyclohexanone	ethylene glycol	none	25	0.25	98	-	20

[a] TON (turnover number) = mole of corresponding product/ mole of catalyst used; [b] *m*PMF: mesoporous poly-melamine-formaldehyde; [c] SO_3H-FSM: propyl-sulfonic acid-functionalized FSM-16 mesoporous silica; [d] M-ZrPO: mesoporous zirconium oxophosphate; [e] mesoporous silica SBA-15 with sulfonic acid (-SO_3H) groups; [f] aprotic imidazolium ionic liquid; [g] IL-silica-polymer: silica-polymer core–shell microspheres with imidazolium-styrene copolymer shells; [h] m-SZ: mesoporous sulfated zirconia.

TON for H-SiW_{12}/SiO_2-catalyzed acetalization of benzaldehyde with 1,3-propanediol is the highest among previously reported values. At the same time, the reaction time is much shorter than that of *m*PMF[11] (Table 5, Entry 3).

To confirm the catalysis of H-SiW_{12}/SiO_2 is truly heterogeneous, acetalization of benzaldehyde with 1,3-propanediol has been carried out using H-SiW_{12}/SiO_2 as catalyst at 60 °C under solvent-free conditions. When the yield reaches about 50%, the solid POM catalyst of H-SiW_{12}/SiO_2 is removed from the reaction mixture by filtration and the reaction is allowed to proceed with the filtrate under the same conditions. No additional corresponding acetal is obtained even re-adding 1,3-propanediol. Furthermore, the ICP analysis of reaction filtrate after acetalization of benzaldehyde with 1,3-propanediol catalyzed by H-SiW_{12} reveal the contents of Si and W are both below 0.01 ppm, respectively (Table S8). The ICP results clearly show that H-SiW_{12} on SiO_2 is not dissolved in reaction mixture during the catalytic reaction, which means the H-SiW_{12}/SiO_2 is not leaching during the reaction. These results rule out the contribution of Si and W species leached into the reaction solution for the observed catalytic results. Similar catalytic results can be achieved with H-SiW_{12}/SiO_2 as catalyst in the acetalization of cylclohexanone with ethylene glycol under solvent-free conditions. The reason is that the interaction with SiO_2 can stabilize H-SiW_{12}. Therefore, the catalysis is truly heterogeneous.

The mechanism of acetalization of aldehydes and ketones with diols (ethylene glycol or 1,3-propanediol) catalyzed by H-SiW_{12} and H-SiW_{12}/SiO_2 has been proposed as follows: (1) the carbonyl group of aldehyde or ketone can be protonated by H-SiW_{12}; (2) the nucleophilic addition to the protonated carbonyl group with one of the hydroxyl groups of diol leads to the corresponding hemiacetal or hemiketal; (3) the intermolecular addition of hemiacetal or hemiketa results in the corresponding acetal or ketal (Figure S4).

4. Conclusions

To summarize, immobilization of H-SiW_{12} onto SiO_2 leads to the formation of the heterogeneous catalyst of H-SiW_{12}/SiO_2. The ^{29}Si CP/MAS NMR and XPS results confirm the presence of the hydrogen bonding interactions between the hydroxyl groups on SiO_2 and the oxygen atoms of the H-SiW_{12}. The surface area of H-SiW_{12}/SiO_2 (324 $m^2{\cdot}g^{-1}$) is much larger than that of H-SiW_{12} (10 $m^2{\cdot}g^{-1}$). The hydrogen bonding interactions and the largely enhanced surface area can reduce the deactivation of strong proton sites.

The heterogeneous catalyst of H-SiW_{12}/SiO_2 can realize selective and efficient acetalization of various aldehydes and ketones with ethylene glycol and 1,3-propanediol under solvent-free conditions at 60 °C. Taking the acetalization of benzaldehyde with 1,3-propanediol as an example, the catalytic reaction proceeds efficiently in 85% yield (benzaldehyde: 1,3-propanediol: H-SiW_{12} = 36000: 54000: 1) under solvent-free conditions with the TON of 30600, which is the highest one reported so far. The H-SiW_{12}/SiO_2 can be recycled at least ten

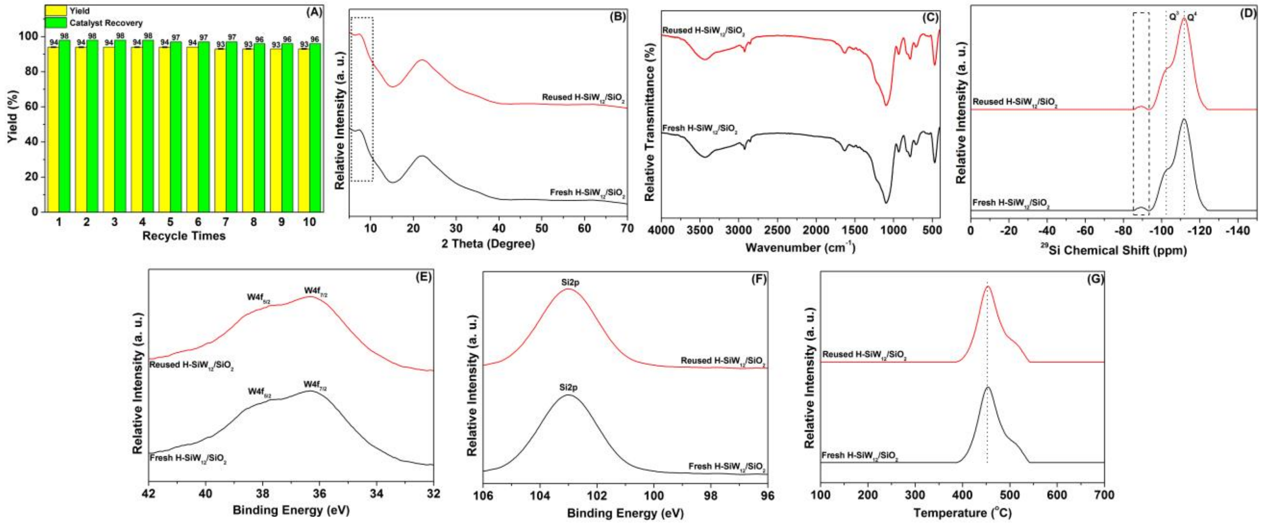

Figure 4. The H-SiW_{12}/SiO_2-recycling and reusing experiments of the acetalization of benzaldehyde with 1,3-propanediol.

times without decrease of catalytic activity. The recycled H-SiW_{12}/SiO_2 remains its structure and composition. The reusability, selectivity and efficiency of H-SiW_{12}/SiO_2 provide great potential for their application in industry.

Acknowledgements

This research was supported by the National Science Foundation of China (21222104), the Fundamental Research Funds for the Central Universities (RC1302) and the Program for Changjiang Scholars and Innovative Research Team in University. Song appreciates the financial support by Key Laboratory of Polyoxometalates Science of Ministry of Education, China.

Notes and references

State Key Laboratory of Chemical Resource Engineering
Beijing University of Chemical Technology
Beijing 100029, P. R. China
Tel/Fax: (+86)10-64431832
E-mail: songyufei@hotmail.com or songyf@mail.buct.edu.cn

† They have the same contribution

Electronic Supplementary Information (ESI) available: The characterization and catalytic results of H-SiW_{12} and H-SiW_{12}/SiO_2. See DOI: 10.1039/b000000x/

1 D. M. Clode, *Chem. Rev.*, 1979, **79**, 491-513.
2 K. Bauer, D. Garbe and H. Surburg, *Common Fragrances and Flavor Materials: Preparation and Uses*, Wiley, New York, 4th edn, 2001.
3 P. G. M. Wuts and T. W. Greene, *Greene's Protective Groups in Organic Synthesis*, Wiley, New York, 4th edn, 2007.
4 F. A. J. Meskens, *Synthesis*, 1981, 501-522.
5 S. A. Patwardhan and S. Dev, *Synthesis*, 1974, 348-349.
6 Y. Dai, B. Li, H. Quan and C. Lü, *Chin. Chem. Lett.*, 2010, **21**, 678-681.
7 K. Shimizu, E. Hayashi, T. Hatamachi, T. Kodama, T. Higuchi, A. Satsuma and Y. Kitayama, *J. Catal.*, 2005, **231**, 131-138.
8 Y. Yamada, K. Qiao, Q. Bao, D. Tomida, D. Nagao, M. Konno and C. Yokoyama, *Catal. Commun.*, 2009, **11**, 227-231.
9 L. Fang, K. Zhang, L. Chen and P. Wu, *Chin. J. Cata.*, 2013, **34**, 932-941.
10 L. Myles, R. Gore, M. Špulák, N. Gathergood and S. J. Connon, *Green Chem.*, 2010, **12**, 1157-1162.
11 M. Tan, L. Gu, N. Li, J. Y. Ying and Y. Zhang, *Green Chem.*, 2013, **15**, 1127-1132.
12 J. S. Swenton, R. M. Blankenship and R. Sanitra, *J. Am. Chem. Soc.*, 1975, **97**, 4941-4947.
13 D. B. G. Williams and M. G. Lawton, *Green Chem.*, 2008, **10**, 914-917.
14 Z. Miao, L. Xu, H. Song, H. Zhao and L. Chou, *Catal. Sci. Technol.*, 2013, **3**, 1942-1954.
15 N. M. Leonard, M. C. Oswald, D. A. Freiberg, B. A. Nattier, R. C. Smith and R. S. Mohan, *J. Org. Chem.*, 2002, **67**, 5202-5207.
16 S. M. Patel, U. V. Chudasama and P. A. Ganesphure, *J. Mol. Catal. A: Chem.*, 2003, **194**, 267-271.
17 Y .W. Zhu, W. B. Yi and C. Cai, *New J. Chem.*, 2013, **37**, 890-892.
18 D. E. Ponde, V. H. Desphande, V. J. Bulbule, A. Sudalai and A. S. Gajare, *J. Org. Chem.*, 1998, **63**, 1058-1063.
19 A. J. Showler and P. A. Darley, *Chem. Rev.*, 1967, **67**, 427-440.
20 A. Sinhamahapatra, N. Sutradhar, M. Ghosh, H. C. Bajaj and A. B. Panda, *Appl. Catal. A: Gen.*, 2011, **402**, 87-93.
21 Special issue on "polyoxometalates", Guest Editor, C. L. Hill, *Chem. Rev.*, 1998, **98**, 1-390.
22 L. Cronin and A. Müller, *Chem. Soc. Rev.*, 2012, **41**, 7333-7334.
23 Y. F. Song and R. Tsunashima, *Chem. Soc. Rev.*, 2012, **41**, 7384-7402.
24 D. L. Long, R. Tsunashima and L. Cronin, *Angew. Chem.*, 2010, **122**, 1780-1803; *Angew. Chem. Int. Ed.*, 2010, **49**, 1736-1758.
25 D. L. Long, E. Burkholder and L. Cronin, *Chem. Soc. Rev.*, 2007, **126**, 117-123.
26 I. V. Kozhevnikov, Catalysis by Polyoxometalates, Wiley, Chichester, 2002.
27 T. Okuhara, N. Mizuno and M. Misono, *Adv. Catal.*, 1996, **41**, 113-252
28 K. A. da Silva, I. V. Kozhevnikov and E. V. Gusevskaya, *J. Mol. Catal. A: Chem.*, 2003, **192**, 129-134.
29 Y. Leng, J. Wang, D. Zhu, X. Ren, H. Ge and L. Shen, *Angew. Chem.*, 2009, **121**, 174-177; *Angew. Chem. Int. Ed.*, 2009, **48**, 168-171.
30 A. L. P. de Meireles, K. A. da Silva Rocha, I. V. Kozhevnikov and E. V. Gusevskaya, *Appl. Catal. A: Gen.*, 2011, **409-410**, 82-86.
31 E. J. L. Lana, K. A. da Silva Rocha, I. V. Kozhevnikov and E. V. Gusevskaya, *J. Mol. Catal. A: Chem.*, 2006, **243**, 258-263.

32 K. A. da Silva Rocha, N. V. S. Rodrigues, I. V. Kozhevnikov and E. V. Gusevskaya, *Appl. Catal. A: Gen.*, 2010, **374**, 87-94.

33 K. A. da Silva Rocha, J. L. Hoehne and E. V. Gusevskaya, *Chem. Eur. J.*, 2008, **14**, 6166-6172.

34 V. V. Costa, K. A. da Silva Rocha, I. V. Kozhevnikov and E. V. Gusevskaya, *Catal. Sci. Technol.*, 2013, **3**, 244-250.

35 K. Shimizu, H. Furukawa, N. Kobayashi, Y. Itaya and A. Satsuma, *Green Chem.*, 2009, **11**, 390-396.

36 Y. Ogasawara, S. Itagaki, K. Yamaguchi and N. Mizuno, *ChemSusChem*, 2011, **4**, 519-525.

37 V. V. Costa, K. A. da Silva Rocha, R. A. Mesquita, E. F. Kozhevnikova, I. V. Kozhevnikov and E. V. Gusevskaya, *ChemCatChem*, 2013, **5**, 3022-3026.

38 A. M. Alexander and R. Neumann, *ChemSusChem*, 2011, **4**, 346-348.

39 Y. Qiao, H. Li, L. Hua, L. Orzechowski, K. Yan, B. Feng, Z. Pan, N. Theyssen, W. Leither and Z. Hou, *ChemPlusChem*, 2012, **77**, 1128-1138.

40 K. S. W. Sing, D. H. Everett, R. A. W. Haul, L. Moscou, R. A. Pierotti, J. Rouquerol and T. Siemieniewska, *Pure Appl. Chem.*, 1985, **57**, 603-620.

41 M. Sun, J. Zhang, Q. Zhang, Y. Wang and H. Wan, *Chem. Comm.*, 2009, 5174-5176.